N termini of apPDE4 isoforms are responsible for targeting the isoforms to different cellular membranes

Deok-Jin Jang, Soo-Won Park, Jin-A Lee, et al.

Learn. Mem. 2010 17: 469-479
Access the most recent version at doi:10.1101/lm.1899410

Research

N termini of apPDE4 isoforms are responsible for targeting the isoforms to different cellular membranes

Deok-Jin Jang,[1,4] Soo-Won Park,[1,4] Jin-A Lee,[2] Changhoon Lee,[1] Yeon-Su Chae,[1] Hyungju Park,[1] Min-Jeong Kim,[1] Sun-Lim Choi,[1] Nuribalhae Lee,[1] Hyoung Kim,[1] and Bong-Kiun Kaang[1,3,5]

[1]*National Creative Research Initiative Center for Memory, Department of Biological Sciences, College of Natural Sciences, Seoul National University, Gwanak-gu, Seoul 151-747, Korea;* [2]*Department of Biotechnology, College of Life Science and Nano Technology, Hannam University, Yuseong-gu, Daejeon 305-811, Korea;* [3]*Department of Brain and Cognitive Sciences, College of Natural Sciences, Seoul National University, Gwanak-gu, Seoul 151-747, Korea*

Phosphodiesterases (PDEs) are known to play a key role in the compartmentalization of cAMP signaling; however, the molecular mechanisms underlying intracellular localization of different PDE isoforms are not understood. In this study, we have found that each of the supershort, short, and long forms of apPDE4 showed distinct localization in the cytoplasm, plasma membrane, and both plasma membrane and presynaptic terminals, respectively. The N-terminal 20 amino acids of the long form of apPDE4 were involved in presynaptic terminal targeting by binding to several lipids. In addition, the N terminus of the short form of apPDE4 bound to several lipids including phosphoinositols, thereby targeting the plasma membrane. Overexpression of the long and the short forms, but not the supershort form attenuated 5-HT-induced membrane hyperexcitability. Finally, the knockdown of apPDE4s in sensory neurons impaired both short-term and long-term facilitation. Thus, these results suggest that apPDE4s can participate in the regulation of cAMP signaling through specific subcellular localization by means of lipid binding activities.

The second messenger cAMP is extremely important for various cellular functions, including synaptic facilitation (Lee et al. 2009). The cAMP signaling cascade modulates synaptic strength and the structure of synapses in the nervous system from invertebrates to mammals (Byrne and Kandel 1996; Davis 1996; Huang et al. 1996). For example, mutation of the *dunce* or *rutabaga* gene, which coded a *Drosophila* PDE4 isoform, or Ca^{2+}/CaM-activated adenylyl cyclase, respectively, disrupted synaptic facilitation and olfactory learning in *Drosophila* (Dudai et al. 1976; Byers et al. 1981; Zhong and Wu 1991).

Phosphodiesterase (PDE) is the only enzyme that can degrade cAMP and cGMP. Among the 11 known families of PDEs, PDE4s have been extensively studied due to the availability of specific inhibitors for PDE4 and its relationship with memory enhancement (Barad et al. 1998; Bourtchouladze et al. 2003). PDE4s are also related to various diseases such as asthma, chronic obstructive pulmonary disease (COPD), and depression (Houslay and Adams 2003; McCahill et al. 2008). Presently, selective or broad-spectrum PDE4 inhibitors have the potential to be used for treating various diseases including asthma and COPD (Spina 2008), and as antidepressants and memory-enhancing agents (Blokland et al. 2006; McCahill et al. 2008).

In mammals, four different PDE4 genes (A, B, C, and D) generate more than 20 different isoforms, which can be classified into three major categories: long, short, and supershort forms. The long form contains three different functional domains: an upstream conserved region 1 (UCR1), UCR2, and the PDE catalytic domain. In contrast to the long form, the short form lacks UCR1, and the supershort form lacks UCR1 and has a truncated UCR2 (Houslay and Adams 2003). Normally, the unique N terminus of a PDE isoform determines its cellular localization through binding with specific proteins or lipids. For example, the N terminus of PDE4D5 interacts with RACK1 (Yarwood et al. 1999) or β-arrestin (Bolger et al. 2003); the N terminus of PDE4D3 interacts with mAKAP (Dodge et al. 2001) or AKAP450 (Tasken et al. 2001); and the N terminus of PDE4B1 interacts with DISC1 (Millar et al. 2005).

Among PDE4s, the brain-specific supershort PDE4A1 is a unique membrane-associated PDE4 that binds with certain types of lipids (Shakur et al. 1993). In PDE4A1, 25 amino acids (aa) of the N terminus are involved in membrane association via two different motifs, namely, helix-1 and helix-2 (Huston et al. 2006). Helix-1 is involved in facilitating membrane association and targeting the *trans*-Golgi network (TGN). Helix-2 contains TAPAS-1, which allows membrane association as it binds with calcium ions and phosphatidic acid (Baillie et al. 2002).

In our previous study, we briefly described the cloning of three apPDE4 isoforms and showed that the long form can target the presynaptic terminals and may play a key role in regulating 5-HT-induced synaptic facilitation (Park et al. 2005). Here, we further characterized the three apPDE4 isoforms and seek to characterize the membrane-targeting mechanisms of the long and short forms of apPDE4. Finally, we examined the effect of overexpression or knockdown of apPDE4s on 5-HT-induced membrane hyperexcitability or synaptic facilitation in *Aplysia*, respectively.

[4]These authors contributed equally to this work.
[5]Corresponding author.
E-mail kaang@snu.ac.kr; fax 82-2-884-9577.
Article is online at http://www.learnmem.org/cgi/doi/10.1101/lm.1899410.

Results

Structure of apPDE4 isoforms

We previously described the cloning process of three apPDE4 isoforms briefly, and focused on studying the roles of apPDE4 long form on 5-HT-induced synaptic facilitation (Park et al. 2005). In this study, we tried to characterize three apPDE4 isoforms further.

First, we examined the molecular structure of apPDE4 isoforms. Based on the comparison of molecular structures between apPDE4s and the mammalian PDE4 family, we categorized apPDE4 isoforms into supershort, short, and long forms. The long form of apPDE4 has a unique N terminus, UCR1/2, and the PDE catalytic domain (Fig. 1A). In contrast, the short form has a unique N terminus, UCR2, PDE catalytic domain, and a truncated UCR1 (Fig. 1A). The supershort form has a unique N terminus, PDE catalytic domain, and a truncated UCR2 (Fig. 1A). Except for the unique N termini, all other overlapping regions have sequences identical to that of the long form, suggesting that these are independent alternative starts. It is notable that each N-terminal region of apPDE4 isoforms has unique sequences that hardly exhibit homology with mammalian PDE4s. The short form of apPDE4 is distinct from that of mammalian PDE4, which does not contain the UCR1 domain, indicating that there may be another apPDE4 isoform corresponding to the short form of mammalian PDE4. Interestingly, the N terminus of the short form of apPDE4 contains a relatively high proportion (14 out of 52) of positively charged amino acids (K/R) (Fig. 1A). This region contains a number of putative phosphorylation sites.

To examine the tissue distribution pattern of each apPDE4 isoform, we performed reverse transcriptase polymerase chain reaction (RT-PCR) with isoform-specific primer sets by using samples obtained from various tissues. As shown in Figure 1B, all three isoforms were primarily expressed in the central nervous system, while their expression was significantly reduced in certain tissues, such as ovotestis and rhinophore. In the case of the short and long forms, a relatively strong band was detected in the pleural ganglion, which contains sensory clusters. On the other hand, the supershort form showed relatively weak expression in the central and pleural ganglia. Taken together, these results indicate that each apPDE4 isoform shows a unique expression pattern in *Aplysia* tissues, including the central nervous system. It might be plausible that the long and the short form are major apPDE4 isoforms in sensory neurons in pleural ganglion.

PDE activity of the apPDE4 isoforms

PDE4s are negative regulators in cAMP signaling that can reduce the intracellular cAMP level (Soderling and Beavo 2000). Although we have cloned three different isoforms of apPDE4 that share a common PDE catalytic domain, the PDE activity can also be modulated according to the type of N-terminal domain. To examine the PDE activity corresponding to each of the apPDE4 isoforms, we performed a PDE4 activity assay. As shown in Figure 2A, the short form of apPDE4 had the lowest K_m value among the three isoforms (K_m values: long form, 7.2 μM; short form, 3.3 μM; supershort form, 34.6 μM).

Next, to examine the functional PDE activity of apPDE4s, we performed a cAMP-responsive element (CRE)-mediated luciferase assay in HEK293T cells. Twenty-four hours after transfection, the cells were treated with 10 μM forskolin (FK) for 3 h. Figure 2B shows the three isoforms having significantly attenuated the CRE-mediated luciferase activity induced by FK treatment (EGFP, 39.78 ± 1.01, $n = 6$; long form, 17.57 ± 3.53, $n = 8$; short form, 9.76 ± 1.30, $n = 8$; supershort form, 21.80 ± 2.54, $n = 8$; each isoform group was compared with the EGFP group [$P < 0.001$], one-way ANOVA; $F = 23.66$, Newman-Keuls test). These results suggested that apPDE4 isoforms show functional PDE activity. In addition, the short form was more efficient than the long or the supershort forms in suppressing the CRE-mediated gene expression induced by FK treatment (short form vs. long form, $P < 0.05$; short form vs. supershort form; $P < 0.01$, one-way ANOVA; $F = 23.66$, Newman-Keuls test), which correlated with the PDE activity shown in Figure 2A.

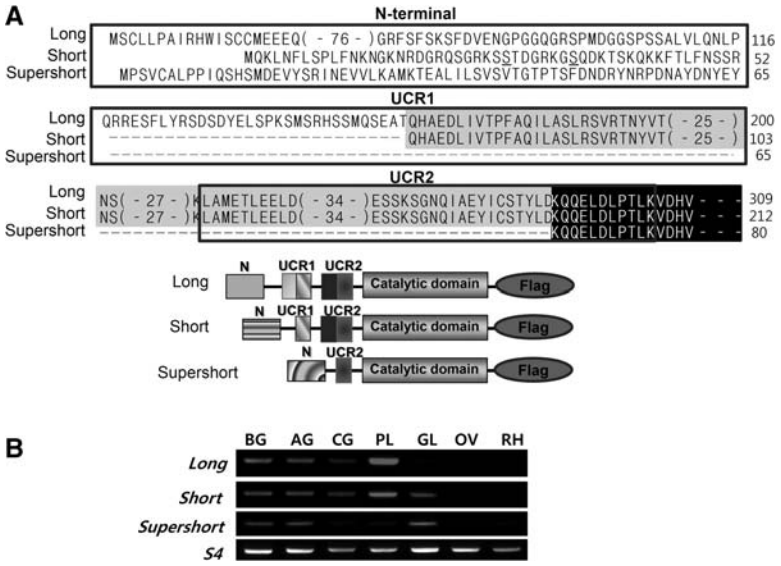

Figure 1. Characterizations of the three apPDE4 isoforms. (*A*) Multiple sequence alignment of the three apPDE4 isoforms. (*Top*) Sequence alignments of the three apPDE4 isoforms. (Underscore) Potential PKA phosphorylation sites (RRXS/T). (*Bottom*) A schematic diagram of the apPDE4 isoforms. The long form of apPDE4 has a unique N terminus, UCR1/2, and the PDE catalytic domain. The short form has a unique N terminus, a truncated UCR1, a complete UCR2, and the PDE-activity domain. The supershort form has a unique N terminus, a truncated UCR2, and the catalytic domain. (*B*) RT-PCR analysis of three apPDE4 isoforms in various tissues. The combination of apPDE4 isoforms expression was analyzed using RT-PCR. S4 was used as a control. (BG) Buccal ganglia; (AG) abdominal ganglia; (CG) central ganglia; (PL) pleural ganglia; (GL) gill; (OV) ovotestis; (RH) rhinophore.

Differences in the cellular localization of the apPDE4 isoforms

We previously showed that the long form was localized at the membrane and presynaptic terminal (Park et al. 2005). However, the cellular localization of the supershort and the short form was not known. Therefore, we determined the cellular localization of the supershort and the short form. Usually, N termini of PDE4s play crucial roles in different cellular targeting (Houslay et al. 2007). Since the supershort and the short forms have obviously different N-terminal sequences compared with that of the long form, we hypothesized that each apPDE4 isoform might be differently localized in *Aplysia* neurons.

To examine this hypothesis, we inserted a 1 × FLAG tag into the C terminus of full-length apPDE4s and ectopically expressed these apPDE4s in the *Aplysia*

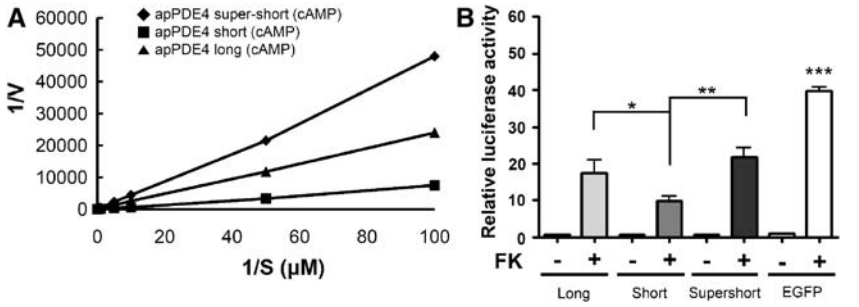

Figure 2. Enzyme activity of the three apPDE4 isoforms. (*A*) A representative plot of substrate specificities of the apPDE4 isoforms. Enzyme activity was determined according to the substrate (cAMP) concentration ranging between 0.1 and 20 μM at eight different concentrations, and the obtained data were fitted to the linear regression function. All three independent experiments demonstrated that apPDE4 hydrolyzed only cAMP and showed cAMP-specific PDE activity. (*B*) Forskolin-induced CRE-mediated luciferase activity in the HEK293T cells expressing apPDE4s. The apPDE4-expressing cells were treated with 10 μM forskolin for 3 h, and the luciferase activity of the treated cells was measured. $^{***}P < 0.001$ compared with each apPDE4 isoform, respectively; $^{**}P < 0.01$; $^{*}P < 0.05$; one-way ANOVA; $F = 23.66$, Newman-Keuls test. The values are presented as the mean ± SEM. (Long) Full length of the long form of apPDE4-1XFLAG; (short) full length of the short form of apPDE4-1XFLAG; (supershort) full length of the supershort form of apPDE4-1XFLAG.

sensory neurons of sensory-to-motor cocultures. First, we confirmed the cellular localization of apPDE4 long form. Consistent with previous results (Park et al. 2005), the long form was expressed at the plasma membrane and colocalized with synaptophysin-EGFP (Syn-EGFP), indicating presynaptic terminal localization (Fig. 3A, top).

On the other hand, the short form was exclusively expressed at the plasma membrane and did not colocalize with Syn-EGFP in synaptic terminals (Fig. 3A, bottom). These results suggested that the short form was mainly expressed at the plasma membrane, which might be mediated by the unique N terminus of the short form.

As shown in Figure 3B (top), the supershort form, which was coexpressed with EGFP, showed diffuse localization in the cytoplasm and neurite. Similarly, the EGFP-apPDE4 supershort form was diffusely expressed in the cytoplasm (Fig. 3B, bottom). Overall, our results clearly showed that each apPDE4 isoform is localized differently within *Aplysia* sensory neurons.

The membrane and presynaptic terminal localization of the long form via the 20-aa segment at the N terminus

Although we have shown that the long form was targeted in the membrane and presynaptic terminal, molecular mechanism of the specific targeting was unclear. To address this, we first examined whether the presence of the N terminus of the long form was sufficient for presynaptic terminal targeting in S-M coculture. As a result, the FLAG-tagged N terminus of the long form was clearly colocalized with Syn-EGFP in S-M cocluture (Fig. 4A).

To further map the membrane and presynaptic terminal targeting site of the long form, we generated deletion-mutant constructs of the EGFP-tagged long form. As shown in Figure 4B, EGFP fusion of the N terminus of the long form showed a similar expression pattern with the FLAG-tagged apPDE4 N terminus shown in Figure 4A, suggesting that EGFP fusion has no effect on the proper targeting.

Next, we examined the cellular localization of the deletion mutants. As shown in Figure 4, B and F, 20 aa of the N terminus of the long form was localized at the membrane and presynaptic terminal in *Aplysia* sensory neurons. This membrane targeting was not restricted to *Aplysia* neurons, as it was localized at the plasma membrane in HEK293T cells (Fig. 4D). Interestingly, apPDE4 L(N20)-EGFP was also localized at intracellular structures in HEK293T cells, as shown in Figure 4, C and D. To identify the intracellular structures, we coexpressed apPDE4 L(N20)-EGFP with hCERT(PH)-mRFP, which can bind to phosphoinositol-4-phosphate (PI4P) and localize at the *trans*-Golgi network (TGN) (Hanada et al. 2003). Interestingly, apPDE4 L(N20)-EGFP was colocalized with hCERT(PH)-mRFP (Fig. 4C), indicating that the long form was localized at TGN in HEK293T cells. On the other hand, apPDE4 L(ΔN20/N)-EGFP was diffusely expressed in

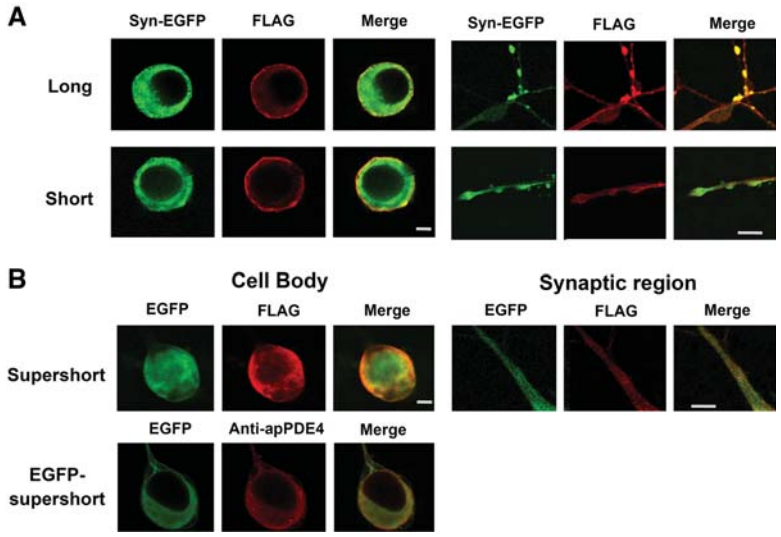

Figure 3. Different cellular localization of the three apPDE4 isoforms in the cultured sensory neurons. (*A*) The long or the short form of apPDE4-1 × FLAG was coexpressed with synaptophysin-EGFP (Syn-EGFP) in sensory neurons of an S-M coculture. The long form was targeted to plasma membrane and cytoplasmic regions partially colocalized with syn-EGFP (*top*, *left*). In synaptic regions, the long form was expressed at plasma membrane and puntate spots, which were perfectly colocalized with syn-EGFP (*top*, *right*). The short form was mainly localized at plasma membrane in both cell body and synaptic region (*bottom*). (*B*) Cytoplasmic localization of the supershort form. Fluorescent images showed the cytoplasmic distribution of the supershort form in sensory cells. (*Top*) The supershort form of apPDE4-1 × FLAG was coexpressed with pNEXδ-EGFP in sensory neurons of an S-M coculture. (*Bottom*) pNEXδ-EGFP-apPDE4 was expressed in cultured sensory cells. The EGFP fusion proteins were stained with an antibody against apPDE4 and Cy3-conjugated anti-mouse antibody 24 h after microinjection. (Long) Full-length derivative of the long form apPDE4-1 × FLAG; (short) full-length derivative of the short form apPDE4-1 × FLAG; (supershort) full-length derivative of the supershort form apPDE4-1 × FLAG. Scale bar, 40 μM.

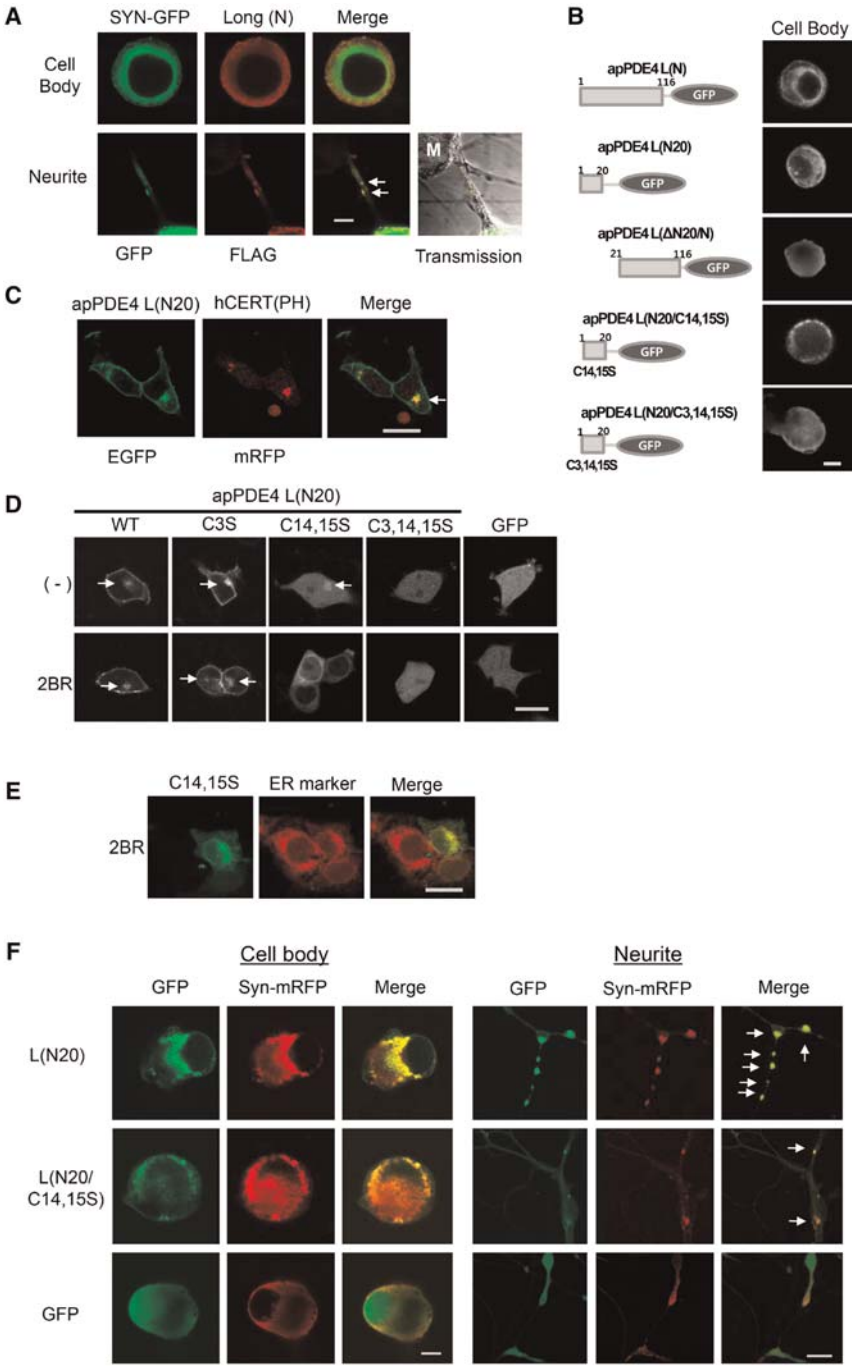

Figure 4. Plasma membrane and TGN localization of the long form via the 20-aa segment of the N-terminal domain. (*A*) The N terminus of the long form of apPDE4-1× FLAG was coexpressed with Syn-EGFP in sensory neurons of an S-M coculture. The N terminus of the long form was colocalized with Syn-EGFP in synaptic varicosity in sensory neurons (white arrows). (M) Motor neuron. Scale bar, 40 μM. (*B*) Localization of the deletion mutants of the long form apPDE4-EGFP in *Aplysia* sensory neurons. The mutant constructs including the N-terminal 20 aa were localized at discrete patterns, including plasma membrane in the cells. On the other hand, apPDE4 L(Δ20/N) and apPDE4 L(N20/C3,14,15S) were diffusely expressed at the cells. Scale bar, 40 μM. (*C*) Cellular localization of the long forms of apPDE4 L(N20)-EGFP in HEK293T cells. hCERT(PH)-EGFP was coexpressed to mark TGN in HEK293T cells. apPDE4 L(N20)-EGFP was localized at the plasma membrane and TGN. A white arrow indicates TGN localization. Scale bar, 20 μM. (*D*) Cellular localization of the mutants of the long form of apPDE4-EGFP in HEK293T cells. To inhibit palmitoylation, the cells were treated with 100 μM 2BR for >6 h. Similar to WT, the C3S mutant was localized at both the plasma membrane and TGN. On the other hand, the C14,15S mutant was expressed mainly at TGN. The C3,14,15S mutant was diffusely expressed at the cells. In the presence of 2BR, the C14,15S mutant was shifted from TGN to cytoplasmic regions. White arrows indicate TGN localization. apPDE4 L(N20), long-form apPDE4 (N20)-EGFP; hCERT(PH), hCERT(PH)-mRFP; WT, long-form apPDE4 (N20)-EGFP; C3S, long-form apPDE4 (N20/C3S)-EGFP; C14,15S, long-form apPDE4 (N20/C14,15S); C3,14,15S, long-form apPDE4 (N20/C3,14,15S). Scale bar, 20 μM. (*E*) ER localization of the C14,15S mutant after 2BR treatment in HEK293T cells. The C14,15S mutant was colocalized with ER marker, calnexin after 100 μM 2BR treatment in HEK293T cells. Scale bar, 20 μM. (*F*) Colocalization of the WT or the C14,15S mutant of the long form with Syn-mRFP in *Aplysia* sensory neurons. White arrows indicate colocalization of EGFP constructs with Syn-mRFP in distal regions of *Aplysia* sensory neurons. L(20), long form apPDE4 (N20)-EGFP; L(N20/C14,15S), long form apPDE4 (N20, C14,15S)-EGFP. Scale bar, 40 μm.

Aplysia sensory neurons (Fig. 4B), suggesting that the 20-aa segment of the N terminus of the long form was sufficient for the proper targeting.

Involvement of cysteine residues in the membrane localization within 20 aa of the long form

How can the 20-aa segment (MSCLLPAIRHWISCCMEEEQ) of the long form be localized at the membrane and presynaptic terminals? To address this, we generated the mutant construct, in which all of the cysteine residues were replaced with serine residues (C3,14,15S), because cysteine is normally involved in protein function due to the thiol group in the side chain. As shown in Figure 4, B and D, the replacement of cysteine residues 3, 14, and 15 by serine residues completely impaired membrane localization in *Aplysia* sensory neurons and HEK 293T cells. These results suggested that the cysteine residues were critical for the membrane targeting.

Next, we asked whether palmitoylation was involved in this localization, because N-terminal cysteine residues can be palmitoylated. Palmitoylation increases hydrophobicity of proteins and induces their incorporation into membrane (El-Husseini and Bredt 2002). To address this, a palmitoylation inhibitor, 100 μM 2-bromo-palmitate (2BR), was applied to apPDE4 (N20)-EGFP expressing HEK293T cells (Fig. 4D). However, 2BR had no effect on the targeting, suggesting that palmitoylation was not involved in this localization. Instead, other modifications in the amino acid sequence or a tertiary structure change might affect targeting.

Next, to examine the role of each cysteine residue, we replaced the third cysteine residue with serine and generated a C3S mutant. However, regardless of the change, the C3S mutant was localized at the plasma membrane and TGN in HEK293T cells (Fig. 4D). 2BR also had little or no effect on the localization. These results suggested that the change in the third cysteine residue was not critical for the targeting.

Next, we replaced the 14th and 15th cysteine residues with serine residues and generated the C14,15S mutant. As shown in Figure 4D, the C14,15S mutant showed patch expression within cytoplasm in *Aplysia* sensory neurons. Interestingly, this mutant was localized at TGN, but not plasma membrane, in HEK293T cells (Fig. 4D). We also examined the presynaptic terminal targeting of this C14,15S mutant. As shown in Figure 4F, this mutant also colocalized with Syn-EGFP in *Aplysia* sensory neurons, suggesting that the C14,15S mutant did not lose the capability of presynaptic terminal targeting in *Aplysia* sensory neuron and TGN localization in HEK293T cells. Therefore, these results suggested that these 14th and 15th cysteine residues contributed to the plasma membrane localization of the long form. In addition, TGN localization of the long form in HEK293T cells seems correlated with presynaptic terminal targeting in *Aplysia* sensory neurons.

Interestingly, the C14,15S mutant was affected by 100 μM 2BR, which allowed a change in localization from TGN to cytoplasm (Fig. 4D). Although we did not detect palmitoylation directly, it is plausible that C3 can be palmitoylated, and this palmitoylation was involved in proper targeting in the C14,15S mutant. To verify where the C14,15S mutant could be localized after 2BR treatment, an ER marker, calnexin was costained with the C14,15S mutant after 2BR treatment. As shown in Figure 5, cytoplasmically distributed, the C14,15S mutant was colocalized with calnexin, suggesting that depalmitoylation of C3 residue in the C14,15S mutant allowed relocation from TGN to ER.

Taken together, these results suggest that 20 aa of the long form were sufficient for the membrane and presynaptic terminal targeting, and changes in C3, 14, and 15 residues within 20 aa altered the specificity of the long-form subcellular localization. Specially, C14 and 15 cysteine residues were involved in the plasma membrane localization. Moreover, the C14,15S mutant was relocated from TGN to ER in a palmitoylation-dependent manner.

Plasma membrane localization of the short form via the N terminus

Next, we asked which sites of the short form were involved in plasma-membrane localization. To address this, we generated apPDE4 short (N-UCR1-2)-EGFP and short (N52)-EGFP, and overexpressed these constructs in *Aplysia* sensory neurons. As shown in Figure 5A, the N terminus of the short form was a key factor in plasma-membrane localization in *Aplysia* sensory neurons. We also confirmed the plasma membrane localization of the N terminus of the short form in HEK293T cells (Fig. 5B), indicating the presence of a common targeting mechanism for plasma-membrane localization in both *Aplysia* neurons and HEK293T cells.

To further map the membrane localization site, we constructed several deletion mutants as shown in Figure 5B and expressed it into HEK293T cells. Serial deletion mutants including N20 and ΔN20/N-UCR1-2 was diffusely expressed in the cells (Fig. 5B), suggesting that full length of the N terminus (N52) were involved in plasma membrane targeting. Meanwhile, the

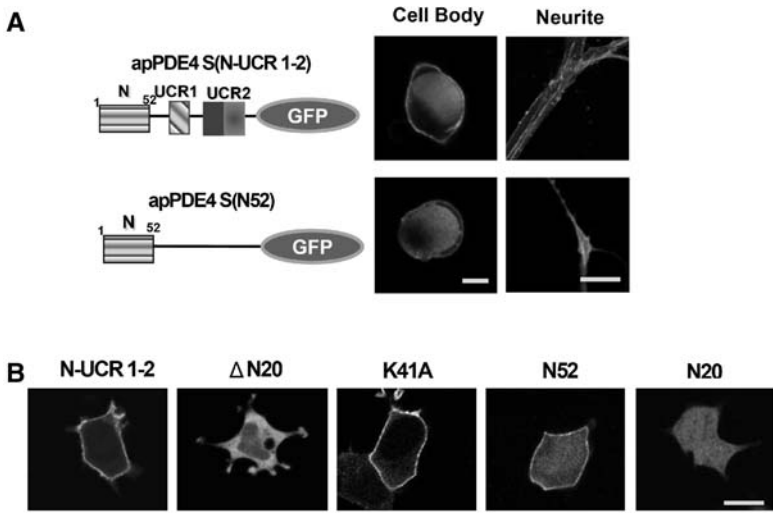

Figure 5. Cellular localization of the N terminus of the short form. (*A*) Plasma membrane localization of the deletion mutants of the short form in *Aplysia* sensory neurons. The N terminus of the short form was sufficient for the plasma membrane localization in sensory cells. (*B*) Cellular localization of the mutants of the short form in HEK293T cells. The mutant constructs including N52 were sufficient for plasma membrane localization. apPDE4 S(N-UCR1-2), short-form apPDE4 (N-UCR1-2)-EGFP; apPDE4 S(N52), short-form apPDE4 (N52)-EGFP; N20, short-form apPDE4 (N20)-EGFP; ΔN20, short-form apPDE4 (ΔN20/N-UCR1-2)-EGFP; and K41A, short-form apPDE4 (N-UCR1-2, K41A)-EGFP. Scale bar, 20 μM.

membrane fluorescence appears less intense in short (N52)-EGFP in the N52 construct compared with that of short (N-UCR1-2)-EGFP in HEK293T cells (Fig. 5B). These results suggested that although the N terminus of the short form plays a critical role in plasma-membrane targeting, UCR1-2 also partially contributes to the plasma-membrane localization.

The alignment of amino acid sequences revealed putative conserved PI-binding sites (apPDE4 short form, $K_{38}TSK_{41}QKKFTLF$; consensus sequence, K-X_n-(K/R)-X-R) (Lemmon 2008). Therefore, to examine whether this motif was involved in plasma membrane localization, we generated a point mutation, K41A. However, a point mutant, apPDE4 S(N-UCR1-2, K41A) showed plasma membrane localization (Fig. 5B), suggesting that plasma membrane targeting of the short form was not mediated by this site.

Lipid binding by the short and long forms of apPDE4

How can apPDE4 short or long form be targeted to the different cellular membranes? We hypothesized that direct lipid binding might be involved in the membrane localization. To test this hypothesis, we performed a lipid-binding assay using lipid membranes. To this end, we generated a 3×FLAG construct containing N-UCR1/2 of the short and long forms of apPDE4, because the presence of the N-UCR1/2 region is sufficient for membrane targeting. We purified the fusion protein in HEK293T cells through FLAG immunoprecipitation. As a negative control, we used 3×FLAG peptides with nontransfected lysates that served as nonspecific FLAG immunoprecipitation products.

First, we observed that the long form is able to bind cardiolipin, sulfatide, and PI4P (Fig. 6). Interestingly, this lipid binding was impaired in the C3,14,15S mutants of the long form. This result was consistent with the cellular localization of the constructs shown in Figure 5D. Thus, C3,14,15S mutation resulted in impairment of lipid binding and membrane association.

In contrast, as shown in Figure 6, the short form can strongly bind to sulfatide, cardiolipin, PI4P, and PI3,4,$5P_3$, and shows less strong, but significant binding to PI4,$5P_2$. In addition, the short form also showed a weak interaction with phosphatidyl acid (PA), phosphatidyl serine (PS), and phosphatidyl glycerol (PG), suggesting that the short form can bind to several PIs in vitro. Therefore, it is plausible that the N terminus of the short and long form of apPDE4 can bind to several types of lipids, thereby leading to plasma-membrane targeting.

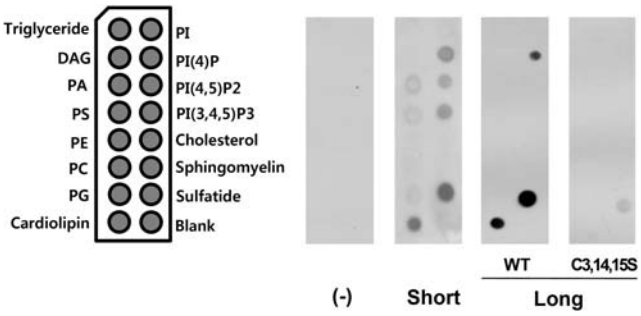

Figure 6. Lipid-binding characteristics of the purified short or long form apPDE4-3×FLAG in vitro. After the construction of N-UCR1-UCR2 of the short or the long form apPDE4 fused to 3×FLAG into the C terminus of pcDNA3.1-3×FLAG vector, proteins were expressed in HEK293T cells and purified by FLAG IP. Membrane-lipid strips were incubated with 0.1 μg/mL of the purified proteins overnight at 4°C. (WT) Long form apPDE4 (N-UCR2)-3×FLAG; (C3,14,15S) long form apPDE4 (N-UCR2/C3,14,15S)-3×FLAG; (short) short form of apPDE4 (N-UCR2)-3×FLAG.

Effects of overexpression of each apPDE4 isoform on 5-HT-induced increase in membrane excitability in *Aplysia* sensory neurons

As shown above, each apPDE4 isoform showed different PDE activity and was expressed differently within sensory neurons. Usually, the neurotransmitter 5-HT up-regulates cAMP levels within sensory cells via Gs coupled 5-HT receptors, activates PKA, and eventually increases the membrane excitability mediated by the closure of S-type K^+ channels (Byrne and Kandel 1996). Therefore, we examined whether overexpression of each apPDE4 isoform actually regulates membrane excitability via regulation of cAMP level in *Aplysia* sensory neurons.

To do this, each pNEXδ-apPDE4 isoform was overexpressed in cultured sensory neurons with pNEXδ-EGFP, a marker of the ectopic expression. We examined the effect of overexpressed apPDE4 isoforms on 5-HT-induced increase in membrane excitability. A single spike was generated by injecting a minimal depolarization current for 500 msec into a sensory neuron. Treatment of sensory neurons overexpressing each isoform with 10 μM 5-HT for 1 min produced a change in the number of spikes (EGFP, 9.45 ± 2.11, $n = 11$; long form, 17.57 ± 3.53, $n = 9$; short form, 3.00 ± 1.16, $n = 7$; supershort form, 6.89 ± 1.14, $n = 8$; $P < 0.05$, one-way ANOVA; $F = 3.73$) (Fig. 7). The 5-HT-induced increase in spike numbers in the cells expressing either the short or the long form was significantly lower than that of sensory neurons expressing EGFP alone (short form vs. EGFP, $P < 0.05$; long form vs. EGFP; $P < 0.05$, one-way ANOVA; $F = 3.73$, Newman-Keuls test). On the contrary, the sensory cells overexpressing the supershort form did not show any significant difference compared with the EGFP-expressing group (supershort form vs. EGFP, $P > 0.05$, one-way ANOVA; $F = 3.73$, Newman-Keuls test). These results show that the short and the long forms but not the supershort form efficiently attenuate 5-HT-induced membrane hyperexcitability in *Aplysia* sensory neurons.

Effect of knockdown of apPDE4s by RNA interference on short- and long-term plasticity in *Aplysia* sensory-to-motor synapses

Next, we examined the effect of knockdown of apPDE4s on synaptic facilitation. To examine the role of cAMP regulation by apPDE4s on synaptic plasticity, first we investigated the effect of 5-HT-induced synaptic facilitation by inhibiting all apPDE4 expressions. For this purpose, we blocked all apPDE4 isoforms expression by microinjecting double-strand RNA of apPDE4 PDE catalytic domain into sensory neurons of sensory-to-motor synapse. This was possible because all isoforms shared the identical PDE catalytic domain. We previously reported that double-strand RNA inhibited specific gene expression in *Aplysia* neurons (Lee et al. 2001).

First, we confirmed that apPDE4 expressions could be effectively blocked by RNA interference (RNAi) by performing immunocytochemistry. When apPDE4 dsRNA was coinjected with EGFP as an injection marker in sensory neuron, endogenous apPDE4s were no longer detected (Fig. 8A).

Next, we determined the effect of inhibiting apPDE4s using RNAi on synaptic facilitation in *Aplysia* sensory to motor synapse by microinjecting apPDE4s dsRNA in sensory neurons of sensory-to-motor synapses. First, we examined the effect of knockdown of apPDE4s on basal synaptic transmission in these cultures. The introduction of apPDE4 dsRNA to sensory neurons had no significant effect on basal synaptic strength (percent change, $-15.7 \pm 11.3\%$, $n = 8$), which was comparable to that of EGFP-expressing cells ($-3.6 \pm 2.9\%$, $n = 12$).

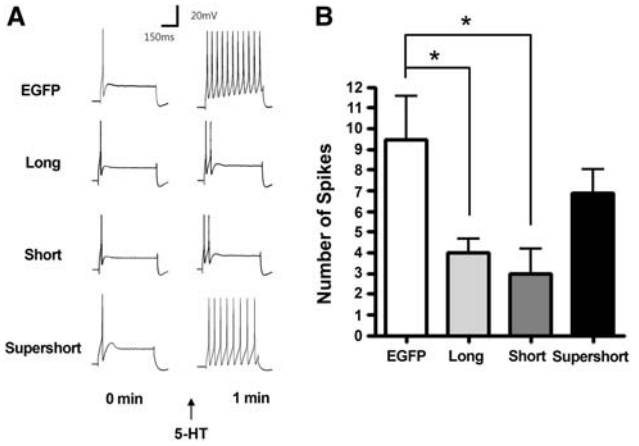

Figure 7. Effects of apPDE4s overexpression on 5-HT-induced membrane hyperexcitability in cultured sensory neurons. 5-HT-induced membrane hyperexcitability was reduced by overexpression of the long or the short form, but not the supershort form. (*A*) Membrane excitability was measured before (0 min) and 1 min after treatment. (*B*) Group data showed that overexpression of the long or the short form but not the supershort form significantly attenuated 5-HT-induced increase in membrane excitability compared with that in EGFP-expressing sensory cells. Membrane excitability is described as the numbers of spikes (action potentials) produced by a fixed-step command over a period of 500 msec. (Long) Full-length derivative of the long form apPDE4-1 × FLAG; (short) full-length derivative of the short form apPDE4-1 × FLAG; (supershort) full-length derivative of the supershort form apPDE4-1 × FLAG. Data are presented as the means ± SEM. $^*P < 0.05$; one-way ANOVA, $F = 3.73$, Newman-Keuls test.

Next, we investigated the effect of inhibiting apPDE4s expression by RNAi on short-term synaptic facilitation. To induce short-term facilitation, the sensory-to-motor coculture was exposed to a single pulse (5 min) of 10 μM 5-HT 24 h after apPDE4 dsRNA microinjection. Interestingly, we found that the cells injected with apPDE4 dsRNA failed to produce a normal short-term facilitation (percent change, 28.7 ± 9.0%, $n = 9$; $P < 0.001$ compared with the EGFP-expressing group, unpaired *t*-test) (Fig. 8B). However, only the EGFP-expressing cells exhibited a normal short-term facilitation (percent change, 93.2 ± 8.5%, $n = 16$). These data indicate that inhibition of apPDE4s can disrupt short-term facilitation.

Finally, to determine the effect of knockdown of apPDE4s expression on long-term facilitation, the sensory-to-motor coculture was exposed to five spaced pulses (5 min) of 10 μM 5-HT, which would normally produce a long-term facilitation 24 h after apPDE4 dsRNA application. The cells that were injected with apPDE4 dsRNA did not produce long-term facilitation (percent change, 15.8 ± 16.5%, $n = 9$; $P < 0.01$ compared with the EGFP-expressing group, unpaired *t*-test), whereas EGFP-expressing cells showed long-term facilitation with a normal increase (percent change, 85.5 ± 11.6%, $n = 16$) (Fig. 8B). These data showed that disruption of apPDE4s could impair long-term facilitation. Taken together, these results suggest that blocking of apPDE4s could impair 5HT-induced short- and long-term facilitation, possibly by disrupting cAMP signaling.

Discussion

In the previous report, we provided brief descriptions of the cloning of three apPDE4 isoforms and the localization of the long form to the presynaptic terminals (Park et al. 2005). However, the molecular mechanism of the presynaptic terminal targeting was unclear. Here, we first further characterized cell-specific expression and PDE activity of the three apPDE4 isoforms. Second, we showed that a 20-aa segment of the long form could be targeted to the membrane and presynaptic terminals. Third, we showed that the plasma membrane localization of the short form occurs via the N terminus, which can bind to several lipids. Fourth, we showed that overexpression of the long or short form, but not the supershort form, reduced 5-HT-induced increase in membrane excitability. Finally, we showed that the knockdown of apPDE4s insensory neurons impaired both short- and long-term facilitation. Thus, each apPDE4 isoform was targeted to different cellular membranes via lipid binding, and this might be responsible for the different cellular regulation of cAMP signaling in *Aplysia*.

Targeting of the membrane and presynaptic terminals by the 20-aa segment of the N terminus of the long form through specific lipid binding

Our results clearly showed that the presence of a 20-aa segment of the long form is sufficient for targeting to the membrane and presynaptic terminal (Fig. 4). How can 20 aa of the long form be targeted to the membrane and presynaptic terminal? To be targeted to the specific membrane, proteins should have the general membrane-association domain and the specific targeting domain. For example, in the case of GAD65, a presynaptic targeting protein, 24–31 aa are required for membrane association and 1–23 aa contain a Golgi localization signal that is necessary for synaptic targeting (Kanaani et al. 2002). In mammalian PDE4, 25 aa of the N terminus of PDE4A1 is involved in membrane association via two helix motifs (Huston et al. 2006). Within the Helix-1 domain it contains targeting sequence to TGN. Interestingly, sequence analysis of the long form suggests the potential amphipathic alpha-helix regions within the N terminus (aa 3–15 [MS**C$_3$LLPAIRHWIS$_{13}$**CC]; DNASTAR). This analysis suggests the possibility of the direct membrane association of the 20-aa segment of the long form. In addition, this peptide showed the specific lipid binding. Interestingly, the N-UCR1/2 domain of the long form can bind to several types of lipids, including PI4P, cardiolipin, and sulfatide (Fig. 6). This lipid binding appeared to be dependent on sequence-specific manners within the 20-aa segment at the N terminus, because the C3,14,15S mutant was nonfunctional (Fig. 6). Thus, considering the cytoplasmic localization of the C3,14,15S mutant, cysteine residues within the 20-aa segment are involved in both membrane association and the specific lipid binding. Usually, PI4P can be used as a lipid marker for TGN (Di Paolo and De Camilli 2006), and sulfatide, one of the glycosphingolipids, is involved in apical trafficking in epithelial cells (Delacour et al. 2005). Therefore, it is possible that these lipid bindings play key roles in TGN and the presynaptic terminal targeting of the long form.

Palmitoylation of the N-terminal 20 aa of the long form might be marginally involved in the proper targeting. The C14, 15S mutant redistributed the localization from TGN to ER in 2BR treatment. This result suggests that palmitoylation of the C14,15S mutant is involved in TGN targeting. C3 is the only cystein within the mutant peptide. Therefore, C3 might be palmitoylated. Indeed, these results were similar to the results obtained for GAD65 (Kanaani et al. 2008), which is a palmitoylation-dependent, presynaptic terminal-targeting protein. In the presence of 100 μM 2BR, the GAD65 expression shifted from TGN to both endoplasmic reticulum (ER) and Golgi apparatus (Kanaani et al. 2008). It has been believed that palmitoylation of the proteins leads to their incorporation into lipid rafts. A number of presynaptic cluster-targeting proteins are palmitoylated (El-Husseini and Bredt 2002). For example, the N terminus of GAP43 has two palmitoylation sites that are involved in presynaptic cluster targeting via lipid raft targeting. Thus, at least in the C14,15S

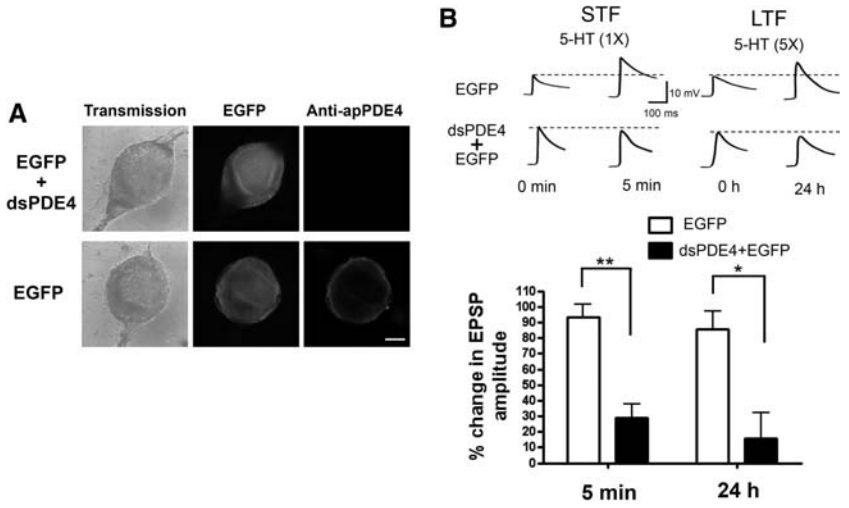

Figure 8. Effect of knockdown of apPDE4s on synaptic facilitation in the sensory-motor synapse. (*A*) apPDE4 dsRNA were coinjected with EGFP as injection marker into cultured sensory neurons. The neurons were fixed and stained with anti-apPDE4 antibody and Cy3-conjugated anti-mouse antibody 24 h after microinjection. EGFP cells represents only the EGFP-injected cells without apPDE4 dsRNA. Endogenous apPDE4 protein was no longer detected in sensory neurons by inhibition of apPDE4 expressions using RNAi. Scale bar, 40 μM. (*B*) Injection of apPDE4 double-strand RNAs blocked both short-term and long-term facilitation, whereas EGFP-expressing cells produced a normal synaptic facilitation. Bar graph represented the effect of apPDE4 dsRNA on short-term and long-term facilitation. For short-term facilitation, EPSP was recorded right after a single 5-HT treatment for 5 min. For long-term facilitation, EPSP was recorded 24 h after five spaced 5-HT treatments for 5 min at 15-min intervals. The height of each bar corresponds to the mean percentage ± SEM in EPSP amplitude tested after 5-HT treatment. (dsPDE4) apPDE4 double-strand RNA; (STF) short-term facilitation; (LTF) long-term facilitation. $^{*}P < 0.01$; $^{**}P < 0.001$; unpaired, two-tailed *t*-test.

mutant, the palmitoylation of C3 plays a key role in TGN targeting in HEK293T cells, probably via lipid raft incorporation.

Plasma membrane localization of the N terminus of the short form via binding with several lipids

Our data showed that the N terminus of the short form was localized at the plasma membrane. A full length of the N terminus is necessary for plasma membrane targeting, because deletion of 20 aa within the N terminus of the apPDE4 short form failed to be localized at the plasma membrane (Fig. 4). Therefore, for proper membrane targeting, a full length of N-terminal domain would be a minimal requirement. Compared with apPDE4 S(N)-EGFP, apPDE4 S(N-UCR1-2)-EGFP was more specifically localized at the plasma membrane. However, UCR1-2 could not be targeted to the membrane, because apPDE4 S(ΔN20/N-UCR1-2)-EGFP failed to localize to the membrane, Indeed, it is widely accepted that UCR1 itself can bind to PA (Grange et al. 2000). Consistent with this, our lipid-binding data also showed PA binding of the short form of apPDE4 (Fig. 6). Collectively, it is possible that UCR1-2 might play a significant role in plasma membrane targeting via PA binding.

Sequence analysis of the short form suggested the potential amphipathic alpha-helix regions within the N terminus (aa 7–12 and aa 18–32; DNASTAR), suggesting a direct membrane binding of the short form. We came to predict the PH-like domains of the short form within the N terminus. Although the short form binds to PIs such as PI4P and PI3,4,5P_3 and shows weak binding to PI4,5P_2, a point mutation of the consensus site (K41A) did not show any different localization with the wild type. These results indicate that membrane localization of the short form is mediated by a different mechanism than the PH-like motif. To our knowledge, this is the first report showing plasma-membrane localization via the N terminus of PDE4. It will be interesting to identify the core-binding sequences of PIs within the N terminus of the short form.

Different roles of apPDE4s in 5-HT-induced membrane hyperexcitability and synaptic plasticity

Our results showed that the long and the short form, which were expressed at the plasma membrane, could reduce 5-HT-induced increase in membrane excitability (Fig. 7). On the contrary, the supershort form, which was expressed in cytoplasm, did not attenuate 5-HT-induced membrane hyperexcitability. This difference in the regulation of membrane excitability could be due to the relative PDE activity of apPDE4s. As shown in Figure 2A, the short and the long form had the higher PDE activity than the supershort form. Therefore, the short and the long form, but not the supershort form, significantly disrupted 5-HT-induced membrane hyperexcitability in *Aplysia* sensory neurons.

Another possibility is that membrane targeting of the short and the long form might efficiently modulate the cAMP level near the plasma membrane, thereby regulating 5-HT-induced membrane hyperexcitability more effectively.

Table 1. List of oligonucleotides and their sequences

Name	Sequence
apPDE4 L(N-UCR2) -XbaI-A	5′-GCTCTAGAGACGTGGTCAACCTTCAG-3′
apPDE L(N20)-XbaI-A	5′-GCTCTAGATTGTTCTTCTTCCATACA-3′
C3S-D3-S	5′-CGAAGCTTGCCACCACCATGTCTTCTTTGCTTCCC GCTATT-3′
C14,15S-XbaI-A	5′-GCTCTAGATTGTTCTTCTTCCATAGAAGAGCTTAT CCAGTGTCT-3′
apPDE4 L(ΔN20)-D3-S	5′-CGAAGCTTGCCACCATGCACGAGCCCCTGCCCGCC-3′
apPDE4 L(N-UCR2) -BamHI-A	5′-CGCGGATCCGACGTGGTCAACCTTCAG-3′
apPDE4 S(N)-XbaI-A	5′-GCTCTAGACCTGGAAGAATTGAAAAG-3′
apPDE4 S(ΔN)-HindIII-S	5′-CGAAGCTTGCCACCACCATGCATGCGGAGGACCTGAT-3′
apPDE4 S(N20)-XbaI-A	5′-GCTCTAGAACCGTCGCGGTTTTTCCC-3′
apPDE4 S(ΔN20)-HindIII-S	5′-GCGAAGCTTGCCACCATGCGACAAAGTGGGAGG-3′
apPDE4 S(K41A)-S	5′-ATAAAACGTCTGCGCAGAAAAAATT-3′
apPDE4 S(K41A)-A	5′-AATTTTTTCTGCGCAGACGTTTTAT-3′
apPDE4 (cat)-A	5′-GTGTGCCGGTCGCACAT-3′
Long-RT-S	5′-CGTCAAGGATTTGGCTGATG-3′
Long-RT-A	5′-GTGTAGCCTCACTCTGCATG-3′
Short-RT-S	5′-GAGGAAGAGTTCAACTGATG-3′
Short-RT-A	5′-AGGATTCATCCGACACCTTG-3′
SShort-RT-S	5′-CTATTCAGTCTCACTCTA TGG-3′
SShort-RT-A	5′-CTTGCTGTTTGTACTCGTAG-3′
S4-S	5′-GACCCTCTGGTGAAGGTGAA-3′
S4-A	5′-TGGACAGCTTCACACC TTTG-3′

Many cAMP signaling molecules such as 5-HT receptor, G-protein, adenylate cyclase, and S-type K^+ channel are membrane proteins. Therefore, membrane localization of apPDE4 isoforms, particularly the long form with cAMP signaling proteins might efficiently enhance the attenuation of 5-HT-induced membrane hyperexcitability. This is the reason why the long form, but not the supershort form, could attenuate 5-HT-induced membrane hyperexcitability significantly (Fig. 7), though both the long and the supershort form could reduce CRE-mediated reporter activity significantly (Fig. 2B).

Acute inhibition of PDE4 by rolipram, a specific PDE4 inhibitor, enhanced LTP and memory acquisition in rodent (Barad et al. 1998). In *Aplysia*, acute treatment of 0.1 μM rolipram in *Aplysia* sensory neuron enhanced membrane excitability (Park et al. 2005). On the other hand, chronic inhibition of PDE4 impaired synaptic plasticity. For example, the *dunce* mutant disrupted synaptic facilitation and olfactory learning in *Drosophila* (Zhong and Wu 1991). In *Aplysia*, chronic treatment of rolipram for 48 h impaired 5-HT-induced cAMP dynamics in *Aplysia* sensory neuron (Park et al. 2005). Consistently, we showed that knockdown of all apPDE4 isoforms in sensory neurons impaired short- and long-term facilitation without affecting basal synaptic transmission (Fig. 8). This disruption of synaptic plasticity might be due to impairment of cAMP dynamics modulated by 5-HT treatment, because knockdown of the long form or chronic treatment of rolipram impaired dynamic change of PKA activation by 5-HT treatment (Park et al. 2005). However, we could not exclude other possibilities due to other modulations such as the regulation of K^+ channel, Ca^{2+} channels, and of synaptic vesicle release. For example, in *Aplysia* sensory neurons, overexpression of *Aplysia* dopamine D1-like receptor, which displays constitutive activity, changed the state of membrane excitability (Barbas et al. 2006). In *dunce* and *rutabaga*, K^+ channel regulation or Ca^{2+} dynamics within the growth cone are disrupted (Alshuaib and Mathew 2002; Berke and Wu 2002). Thus, lots of proteins were affected by chronic impairment of cAMP signaling. In *Aplysia*, K^+ channels, Ca^{2+} channels, and synaptic proteins involved in synaptic vesicle release are modulated by 5-HT treatment (Byrne and Kandel 1996). Therefore, beside the regulation of cAMP dynamics, overexpression or knockdown of apPDE4s might modulate chronic change of K^+ and Ca^{2+} channels activity and the expression of synaptic proteins, eventually leading to disruption of synaptic plasticity.

Materials and Methods

DNA constructs

We used previously described FLAG-fused supershort, short, and long forms of pNEX-apPDE4 (Park et al. 2005). The same Kozac sequence (GCCACCACC) in front of the initiation ATG sequence was added to adjust expression efficiency. The deletion mutants of the long and short forms of apPDE4 were obtained by performing PCR using a specific primer set: apPDE4 L(N), RSV-S/long form apPDE4 L(N)-XbaI-A; apPDE4 L(ΔN20/N), long-form apPDE4 L(ΔN20)-D3-S/long-form apPDE4 (N)-XbaI-A; apPDE4 L(N20), RSV-S/long-form apPDE4 (N20)-XbaI-A; apPDE4 S(N), RSV-S/short-form apPDE4 (N)-XbaI-A; and apPDE4 S(N-UCR1-2), RSV-S/long-form apPDE4 (N-UCR1-2)-XbaI-A; apPDE4 S(ΔN20), Short-form apPDE4 S(ΔN20/N-UCR1-2)-XbaI-S/apPDE4 L(N-UCR2)-XbaI-A; and apPDE4 S(N20), RSV-S/Short form apPDE4 S(N20)-XbaI-A (Table 1). The PCR products were separately subcloned into HindIII–XbaI-digested pNEXδ-enhanced green fluorescent protein (EGFP) to create pNEXδ-apPDE4 mutant-EGFP.

The mutant fragments of the long (N20/C3S), long (N20/C14,15S), or long (N20/C3,14,15S) forms of apPDE4 were generated by recombinant PCR using specific sense and antisense primers (the sense primer contained C3S [C3S-D3-S] and the antisense primer contained C14,15S [C14,15S-*Xba*I-A]). The PCR products were separately subcloned onto HindIII–XbaI–digested pNEXδ-EGFP to create pNEXδ-apPDE4-EGFP mutants. To generate the 3×FLAG constructs, the N-UCR1/2 regions of the long and short forms of apPDE4 were subcloned into HindIII–BamHI-digested pcDNA3.1-3×FLAG vectors.

Mutants of the short-form apPDE4 (K41A) were generated by PCR using apPDE4 S(K41A)-S and apPDE4 S(K41A)-A. The PCR products were subcloned into HindIII–XbaI-digested pNEXδ-EGFP to create pNEXδ-apPDE4 S(K41A)-EGFP mutants.

To clone human ceramide transfer protein (CERT)-pleckstrin homology (PH) domains, we performed polymerase chain reaction (PCR) for the HeLa cDNA library. We used the following primers: RT-S, 5′-GTTGTCGAGCCTCCATGTC-3′; RT-A1, 5′-TGA-AGAGGTGGATGTTGCAG-3′; and RT-A2, 5′-TTGCCGTTGGTA-CTATGCAA-3′. The PCR products were subcloned into the pNEXδ-EGFP vector by using HindIII/XbaI restriction sites.

Cell culture

We isolated *Aplysia* sensory cells from the pleural ganglia of adult animals (100–150 g) and cultured these cells to obtain a sensory-neuron culture. For the sensory-to-motor culture, these cells were cocultured with a left F terminal innervating the siphon (LFS) motor neuron from the abdominal ganglia of adult animals, as described previously (Montarolo et al. 1986; Lee et al. 2001). The cultures were maintained for 3–4 d at 18°C and then used for immunocytochemistry.

The HEK293T cells were grown in Dulbecco's modified Eagle's medium (DMEM) supplemented with 10% (v/v) fetal bovine serum (FBS) and penicillin/streptomycin in a humidified atmosphere of 5% (v/v) CO_2 at 37°C. For the palmitoylation experiments, the cells were treated with 2BR (Sigma), a reversible palmitoylation inhibitor, for more than 6 h to block palmitoylation.

apPDE4 antibody

To generate polyclonal mouse antisera against the PDE catalytic domain of apPDE4s, the gene encoding the catalytic domain of apPDE4 was fused to the downstream region of His-tag in pRSETa vector (Invitrogen). Purified His-apPDE4 fusion protein from *E. coli* was used to immunize the mouse strain Balb/c. Polyclonal anti-apPDE4 antibody was purified from the antisera according to the method described previously (Gruber and Zingales 1995).

Immunocytochemistry

We performed immunocytochemistry as described previously (Park et al. 2005). The monoclonal mouse anti-FLAG antibody (Sigma) and the secondary cyanine 3 (Cy3)-conjugated anti-mouse antibody (Amersham Biosciences) were used as dilution factors of 1:250 and 1:1000, respectively. Anti-calnexin (Abcam) antibody was used as an ER marker in HEK293T cells. We obtained and analyzed fluorescence images by a confocal laser-scanning microscope (Radiance 2000, Zeiss) and NIH Image J software (National Institutes of Health), respectively.

RT-PCR analysis

Total RNA was extracted from tissues using TRIzol Reagent II. The cDNA was synthesized by using Superscript III reverse transcriptase with random hexamers as the primers. These cDNAs were used as templates for PCR reactions for S4 (S4-S/S4-A) and the long (long-RT-S/Long-RT-A), short (Short-RT-S/Short-RT-A), and supershort (SShort-RT-S/SShort-RT-A) forms of apPDE4. Amplification was performed ranging from 27 to 34 cycles (94°C, 15 sec; 60°C, 15 sec; 72°C, 30 sec). The PCR products were visualized on 2% agarose gel.

Immunoprecipitation

For transient transfection, HEK293T cells were plated at a density of $5–7 \times 10^5$ cells per well in 6-well plates and cultured for 24 h.

The cells were then transfected with DNA constructs using Lipofectamine 2000 (Invitrogen) and incubated for 24 h. For FLAG immunoprecipitation, the transfected HEK293T cells were washed twice with 1×phosphate-buffered saline (PBS) and lysed with a buffer containing 1% Triton X-100, 50 mM Tris-HCl (pH 7.5), 150 mM NaCl, 2 mM EDTA, and protease-inhibitor cocktails (Roche). The cell lysate was incubated with 50 μL (bead volume) of mouse anti-Flag M2 antibody conjugated beads (Sigma) at 4°C overnight. Subsequently, the beads were washed three times with the lysis buffer. Finally, the immunoprecipitate was eluted by adding 2 μg/mL of 3×FLAG peptides and analyzed by Coomassie blue staining.

Lipid-binding assay

Membrane strips (Echelon) were used for the in vitro lipid-binding assay. We performed the assay according to the manufacturer's protocol. Briefly, the membrane was blocked with 1% nonfat milk in 1×PBS for 1 h at room temperature and incubated with the purified apPDE4 short or long form (N-UCR1-2)-3×FLAG protein (0.1 μg/mL) in PBS containing 1% nonfat milk. Next, the membrane was incubated with mouse anti-FLAG M2 antibodies (Sigma) for 1 h at room temperature. The bound primary antibodies were treated with a horseradish peroxidase-conjugated goat antimouse IgG (Santa Cruz Biotechnologies) and detected by an electrochemiluminescence-detection system.

Luciferase assays

HEK293T cells were cultured in 12-well plates and cotransfected with 100 ng of TK luciferase, 500 ng of CRE luciferase, 170 ng of long-form apPDE4, and 30 ng of EGFP. For the analysis of short and supershort form apPDE4s, we used 55 ng of short-form apPDE4, 200 ng of supershort-form apPDE4, and 200 ng of EGFP. In the first experiment, we measured the CRE-luciferase activities with or without forskolin treatment. The other experiment was performed with or without cotransfection of the 5-HT receptor genes. After 24 h of transfection, the cells were lysed using lysis buffer (Promega) and assayed using the Promega dual luciferase-assay system. The measurements were performed in a 96-microplate luminometer. The results were normalized using *Renilla* luciferase activities.

PDE activity assay

We assayed the PDE activity by performing a modified version of a previously described procedure (Bauer and Schwabe 1980). This method is based on the conversion of ^{3}H-labeled cAMP to ^{3}H-labeled 5-AMP by phosphodiesterase activity. Degraded ^{3}H-labeled cAMP was purified using QAE-Sephadex (Sigma) columns. We prepared the apPDE4 protein by overexpressing pcDNA3.1-apPDE4-1×FLAG in COS7 cells. We confirmed that the overexpressed apPDE4 proteins primarily existed in the soluble part by performing Western blotting using monoclonal mouse anti-FLAG (Sigma) (data not shown). The assay was carried out in two steps. First, we performed reactions at pH 8.0 in 40 mM Tris-HCl buffer containing 0.5 mM $MgCl_2$, 1 μM [^{3}H]cAMP (80,000 cpm) and diluted apPDE4-overexpressed COS7 cytosolic extract with a final volume of 0.2 mL. We initiated the reaction by adding the extract to the assay mixture; the reaction was performed in a 1.5-mL tube at 30°C for 10 min and terminated by heating the tubes to 95°C for 3 min, which was followed by immediate cooling on ice. In the second step, 50 μL of *Crotalus atrox* snake venom (1 mg/mL) (Sigma) was added for [^{3}H]adenosine formation. After a 10-min incubation at 30°C, we terminated the reaction by applying a 0.2-mL aliquot to the QAE A-25 Sephadex column previously equilibrated with 3 mL of 30 mM ammonium formate (pH 6.0). We collected elutes directly into scintillation vials and measured the radioactivity level in 8 mL of a scintillation fluid. We determined the K_m values over a substrate range of 0.1–20 μM cAMP (eight different concentrations) by fitting the obtained values to the hyperbolic form of the Michaelis-Menten equation by using a least-square procedure provided in the Origin 6 software.

RNA synthesis by in vitro transcription

To make template DNAs for in vitro transcription, the PDE catalytic domain of apPDE4 was inserted into pLITMUS28i vector using BamHI. dsRNA was synthesized by in vitro transcription of linearized template DNAs using T7 RNA polymerase.

Electrophysiology, and the induction of long-term facilitation by 5-HT

The voltage recordings and current injections were carried out as described previously (Chang et al. 2000). For membrane excitability recording, cultured sensory neurons were impaled with a microelectrode (8∼13 MΩ) filled with 0.5 M KCl, 2 M K-acetate, and 10 mM K-HEPES (pH 7.4). The resting potential measured 5–10 min after impalement. Only cells with a resting potential more negative than −40 mV were used. 5-hydroxytryptamine (5-HT) (Sigma) was freshly made by dissolving in L15/ASW. Before measuring membrane excitability, the resting membrane potential was adjusted at −45 mV through current injection. 5-HT-induced change of membrane excitability was measured 1 min after 10 μM 5-HT treatment as the number of action potentials elicited during 500 msec, by a depolarizing current pulse (0.05–0.3 nA), which produced one spike before drug application.

For excitatory postsynaptic potential (EPSP) recording, the motor cell was impaled intracellularly with a glass microelectrode, and the membrane potential was held at −30 mV below its resting value. The EPSP was evoked in LFS by stimulating the sensory neurons with a brief depolarizing stimulus using an extracellular electrode. To examine basal synaptic transmission, the EPSP was measured before and 48 h after microinjection of dsRNA of apPDE4. To investigate the effect of apPDE4 on synaptic plasticity, the initial EPSP value was measured 24 h after microinjection. The cultures then received a single pulse of 5-HT to induce short-term facilitation or five spaced pulses of 5-HT for 5 min at 15-min intervals to induce long-term facilitation. The degree of synaptic facilitation was determined based on the percentage change in EPSP amplitude recorded after the 5-HT treatment versus its initial value before treatment.

Acknowledgments

This work was supported by the National Creative Research Initiative Program of the Korean Ministry of Science and Technology. D.-J. J. and N.L. are supported by a BK21 fellowship.

References

Alshuaib WB, Mathew MV. 2002. Reduced delayed-rectifier K^+ current in the learning mutant *rutabaga*. *Learn Mem* **9:** 368–375.

Baillie GS, Huston E, Scotland G, Hodgkin M, Gall I, Peden AH, MacKenzie C, Houslay ES, Currie R, Pettitt TR, et al. 2002. TAPAS-1, a novel microdomain within the unique N-terminal region of the PDE4A1 cAMP-specific phosphodiesterase that allows rapid, Ca^{2+}-triggered membrane association with selectivity for interaction with phosphatidic acid. *J Biol Chem* **277:** 28298–28309.

Barad M, Bourtchouladze R, Winder DG, Golan H, Kandel E. 1998. Rolipram, a type IV-specific phosphodiesterase inhibitor, facilitates the establishment of long-lasting long-term potentiation and improves memory. *Proc Natl Acad Sci* **95:** 15020–15025.

Barbas D, Zappulla JP, Angers S, Bouvier M, Mohamed HA, Byrne JH, Castellucci VF, DesGroseillers L. 2006. An *aplysia* dopamine1-like receptor: Molecular and functional characterization. *J Neurochem* **96:** 414–427.

Bauer AC, Schwabe U. 1980. An improved assay of cyclic 3′,5′-nucleotide phosphodiesterases with QAE-Sephadex columns. *Naunyn Schmiedebergs Arch Pharmacol* **311:** 193–198.

Berke B, Wu CF. 2002. Regional calcium regulation within cultured *Drosophila* neurons: Effects of altered cAMP metabolism by the learning mutations *dunce* and *rutabaga*. *J Neurosci* **22:** 4437–4447.

Blokland A, Schreiber R, Prickaerts J. 2006. Improving memory: A role for phosphodiesterases. *Curr Pharm Des* **12:** 2511–2523.

Bolger GB, McCahill A, Huston E, Cheung YF, McSorley T, Baillie GS, Houslay MD. 2003. The unique amino-terminal region of the PDE4D5 cAMP phosphodiesterase isoform confers preferential interaction with β-arrestins. *J Biol Chem* **278:** 49230–49238.

Bourtchouladze R, Lidge R, Catapano R, Stanley J, Gossweiler S, Romashko D, Scott R, Tully T. 2003. A mouse model of Rubinstein-Taybi syndrome: Defective long-term memory is ameliorated by inhibitors of phosphodiesterase 4. *Proc Natl Acad Sci* **100:** 10518–10522.

Byers D, Davis RL, Kiger JA Jr, 1981. Defect in cyclic AMP phosphodiesterase due to the *dunce* mutation of learning in *Drosophila melanogaster*. *Nature* **289:** 79–81.

Byrne JH, Kandel ER. 1996. Presynaptic facilitation revisited: State and time dependence. *J Neurosci* **16:** 425–435.

Chang DJ, Li XC, Lee YS, Kim HK, Kim US, Cho NJ, Lo X, Weiss KR, Kandel ER, Kaang BK. 2000. Activation of a heterologously expressed octopamine receptor coupled only to adenylyl cyclase produces all the features of presynaptic facilitation in aplysia sensory neurons. *Proc Natl Acad Sci* **97:** 1829–1834.

Davis RL. 1996. Physiology and biochemistry of *Drosophila* learning mutants. *Physiol Rev* **76:** 299–317.

Delacour D, Gouyer V, Zanetta JP, Drobecq H, Leteurtre E, Grard G, Moreau-Hannedouche O, Maes E, Pons A, Andre S, et al. 2005. Galectin-4 and sulfatides in apical membrane trafficking in enterocyte-like cells. *J Cell Biol* **169:** 491–501.

Di Paolo G, De Camilli P. 2006. Phosphoinositides in cell regulation and membrane dynamics. *Nature* **443:** 651–657.

Dodge KL, Khouangsathiene S, Kapiloff MS, Mouton R, Hill EV, Houslay MD, Langeberg LK, Scott JD. 2001. mAKAP assembles a protein kinase A/PDE4 phosphodiesterase cAMP signaling module. *EMBO J* **20:** 1921–1930.

Dudai Y, Jan YN, Byers D, Quinn WG, Benzer S. 1976. *dunce*, a mutant of *Drosophila* deficient in learning. *Proc Natl Acad Sci* **73:** 1684–1688.

El-Husseini AE, Bredt DS. 2002. Protein palmitoylation: A regulator of neuronal development and function. *Nat Rev Neurosci* **3:** 791–802.

Grange M, Sette C, Cuomo M, Conti M, Lagarde M, Prigent AF, Nemoz G. 2000. The cAMP-specific phosphodiesterase PDE4D3 is regulated by phosphatidic acid binding. Consequences for cAMP signaling pathway and characterization of a phosphatidic acid binding site. *J Biol Chem* **275:** 33379–33387.

Gruber A, Zingales B. 1995. Alternative method to remove antibacterial antibodies from antisera used for screening of expression libraries. *Biotechniques* **19:** 28, 30.

Hanada K, Kumagai K, Yasuda S, Miura Y, Kawano M, Fukasawa M, Nishijima M. 2003. Molecular machinery for non-vesicular trafficking of ceramide. *Nature* **426:** 803–809.

Houslay MD, Adams DR. 2003. PDE4 cAMP phosphodiesterases: Modular enzymes that orchestrate signalling cross-talk, desensitization and compartmentalization. *Biochem J* **370:** 1–18.

Houslay MD, Baillie GS, Maurice DH. 2007. cAMP-specific phosphodiesterase-4 enzymes in the cardiovascular system: A molecular toolbox for generating compartmentalized cAMP signaling. *Circ Res* **100:** 950–966.

Huang YY, Nguyen PV, Abel T, Kandel ER. 1996. Long-lasting forms of synaptic potentiation in the mammalian hippocampus. *Learn Mem* **3:** 74–85.

Huston E, Gall I, Houslay TM, Houslay MD. 2006. Helix-1 of the cAMP-specific phosphodiesterase PDE4A1 regulates its phospholipase-D-dependent redistribution in response to release of Ca^{2+}. *J Cell Sci* **119:** 3799–3810.

Kanaani J, El-Husseini AE, Aguilera-Moreno A, Diacovo JM, Bredt DS, Baekkeskov S. 2002. A combination of three distinct trafficking signals mediates axonal targeting and presynaptic clustering of GAD65. *J Cell Biol* **158:** 1229–1238.

Kanaani J, Patterson G, Schaufele F, Lippincott-Schwartz J, Baekkeskov S. 2008. A palmitoylation cycle dynamically regulates partitioning of the GABA-synthesizing enzyme GAD65 between ER-Golgi and post-Golgi membranes. *J Cell Sci* **121:** 437–449.

Lee JA, Kim HK, Kim KH, Han JH, Lee YS, Lim CS, Chang DJ, Kubo T, Kaang BK. 2001. Overexpression of and RNA interference with the CCAAT enhancer-binding protein on long-term facilitation of *Aplysia* sensory to motor synapses. *Learn Mem* **8:** 220–226.

Lee YS, Choi SL, Lee SH, Kim H, Park H, Lee N, Chae YS, Jang DJ, Kandel ER, Kaang BK. 2009. Identification of a serotonin receptor coupled to adenylyl cyclase involved in learning-related heterosynaptic facilitation in *Aplysia*. *Proc Natl Acad Sci* **106:** 14634–14639.

Lemmon MA. 2008. Membrane recognition by phospholipid-binding domains. *Nat Rev Mol Cell Biol* **9:** 99–111.

McCahill AC, Huston E, Li X, Houslay MD. 2008. PDE4 associates with different scaffolding proteins: Modulating interactions as treatment for certain diseases. *Handb Exp Pharmacol* **186:** 125–166.

Millar JK, Pickard BS, Mackie S, James R, Christie S, Buchanan SR, Malloy MP, Chubb JE, Huston E, Baillie GS, et al. 2005. DISC1 and PDE4B are interacting genetic factors in schizophrenia that regulate cAMP signaling. *Science* **310:** 1187–1191.

Montarolo PG, Goelet P, Castellucci VF, Morgan J, Kandel ER, Schacher S. 1986. A critical period for macromolecular synthesis in long-term heterosynaptic facilitation in *Aplysia*. *Science* **234:** 1249–1254.

Park H, Lee JA, Lee C, Kim MJ, Chang DJ, Kim H, Lee SH, Lee YS, Kaang BK. 2005. An Aplysia type 4 phosphodiesterase homolog localizes at the presynaptic terminals of *Aplysia* neuron and regulates synaptic facilitation. *J Neurosci* **25:** 9037–9045.

Shakur Y, Pryde JG, Houslay MD. 1993. Engineered deletion of the unique N-terminal domain of the cyclic AMP-specific phosphodiesterase RD1 prevents plasma membrane association and the attainment of enhanced thermostability without altering its sensitivity to inhibition by rolipram. *Biochem J* **292:** 677–686.

Soderling SH, Beavo JA. 2000. Regulation of cAMP and cGMP signaling: New phosphodiesterases and new functions. *Curr Opin Cell Biol* **12:** 174–179.

Spina D. 2008. PDE4 inhibitors: Current status. *Br J Pharmacol* **155:** 308–315.

Tasken KA, Collas P, Kemmner WA, Witczak O, Conti M, Tasken K. 2001. Phosphodiesterase 4D and protein kinase a type II constitute a signaling unit in the centrosomal area. *J Biol Chem* **276:** 21999–22002.

Yarwood SJ, Steele MR, Scotland G, Houslay MD, Bolger GB. 1999. The RACK1 signaling scaffold protein selectively interacts with the cAMP-specific phosphodiesterase PDE4D5 isoform. *J Biol Chem* **274:** 14909–14917.

Zhong Y, Wu CF. 1991. Altered synaptic plasticity in *Drosophila* memory mutants with a defective cyclic AMP cascade. *Science* **251:** 198–201.

Received June 9, 2010; accepted in revised form July 8, 2010.